[1,2,6]Krishnakant Mishra
[3,6]Santosh Mani
[4,6]Sameer Hadkar
[5]Ravindra Upadhyay
[6]Pradip Sarawade
[6]S. K Dubey

Effect of Metal Nanoparticle on Optical and Thermal Properties of Liquid Crystal Polymer System

Abstract: - In the present study the optical and thermal properties of a Nematic Liquid Crystal Polymer System (NLCPS) dispersed with different concentrations of metal nanoparticles like ZnO, Zn, CuO were investigated using X-Ray Diffraction (XRD), Differential Scanning Calorimetry (DSC) and Fourier Transform Infra-Red (FTIR). The comparison of various parameters of pure NLCPS and its mixture with different concentrations of dopant was carried out to understand the effect of nanoparticles on the optical and thermal properties of NLCPS. Our investigation shows an increase in phase transition temperature after dispersing the metal nanoparticle. The maximum phase transition temperature was found for ZnO. XRD shows a sharp reflection and diffuse scattering is characteristic of crystalline and amorphous phases of conventional semi-crystalline polymers. The presence of functional groups in the nanoparticle dispersed NLCPS has been identified using Fourier Transform Infrared Spectroscopy (FTIR). The investigation may be useful for various energy-efficient devices in addition to display applications.

Keywords: Nematic Liquid Crystal Polymer System (NLCPS), X-Ray Diffraction (XRD), Fourier Transform Infra-Red (FTIR), Differential Scanning Calorimetry (DSC)

I. Introduction

Liquid crystal (LC) is a fascinating state of matter found between crystalline solid and liquid. The molecules in this state are found to be asymmetric in nature and due to this, LC show regular arrangement in one preferred direction and random in all other directions. They have properties like molecular mobility and fluidity that of a liquid and optical anisotropy, electrical and optical properties that of crystalline solid. These materials are successfully used for all display applications like smartphones, calculators, laptop, tablets and diagnosis of arteries, placenta, tumors, enzymes, nucleic acids, glucose etc. In addition to these applications, they are also found suitable for smart windows, chromatographic separations, optical shuttering action, polarization-converting materials [1-5].

The LC materials due to its molecular order and self-assembly can be used for preparing smart and functional materials which changes its properties due to external stimuli called liquid crystal polymer system (LCPS). They show reversible deformation governed by order–disorder phase transition of molecules and hence used for various applications like responsive pigments, soft robotics, adsorbents, smart textiles, and sensors [6-11, 18-22].

Another important material which brought revolution due to its optical, physical, chemical electrical and mechanical properties are nanomaterials. When these materials are incorporated into LCPS, then due to structural rearrangements, they found to enhance various properties like optical, thermal, electrical etc. The LCPS embedded with metallic nanoparticles have attracted much attention in recent years owing to their prospective applications in various fields. They are more widely used than other display technologies due to their numerous benefits, including low operating voltage, high contrast ratio, quick electro-optical response, simple manufacturing, low-cost production, and ease of processing [12-17, 22-27].

Recently, various researchers have investigated the physical properties of LCPS dispersed with nanomaterials, like cholesteric liquid crystal composites dispersed with titanium oxide nanoparticles were studied by Garima Chauhan at al.[28], the metal oxide induced polymer-dispersed liquid crystal composites were studied by Praveen Malik et al. [29], Lu, Yinfu, et al. studied fluorescent molecules and nanoparticles dispersed with polymer-dispersed liquid crystals [30] and silicon nanostructure with polymer-dispersed liquid crystal were studied by Zhang, Cuihong, et al. [31]. In the present study, the ZnO nanoparticles were dispersed in LCPS, and optical, thermal and structural properties were studied.

[1]Thakur College of Engineering & Technology, Kandivali (East), Mumbai, INDIA
[2]Thakur Specialized Degree College, Kandivali (West), Mumbai, INDIA
[3]K. J. Somaiya College of Engineering, Somaiya Vidyavihar University, Mumbai, INDIA
[4]Don Bosco Institute of Technology, Kurla, Mumbai, INDIA
[5]Maharshi Dayanand College of Arts, Science & Commerce , Parel, Mumbai, INDIA
[6]Department of Physics, University of Mumbai, Santacruz (E), Mumbai, INDIA
krishnakant.mishra@tcetmumbai.in, santoshmani@somaiya.edu, sameerhadkar@dbit.in

II. Formulation

Liquid Crystal Polymer System (LCPS) was produced using 4-Pentyl-4'-Cyano-Biphenyl, Ethylhexyl Acrylate, and Acrylated Oligomer. LCPS was combined with ZnO nanoparticles. ZnO nanoparticles distributed in LCPS were combined uniformly after sonication. The remaining nanoparticles, Zn and CuO, were disseminated in LCPS in a similar manner.

Initial acetone rinsing of the slide and cover slip, followed by wiping with a tissue in a direction parallel to one fixed direction of the slide, were done for the homogenous alignment of the sample [5–11]. The sample is then placed on the slide with a few drops, and the cover slip is slipped over it in the manner described above. A homogeneous mixture of ZnO nanoparticles distributed in LCPS is obtained after sonication and magnetic stirring.

III. Methodology

X-Ray Diffraction Studies: The X-Ray Diffraction (XRD) measurements on the samples were carried out on Bruker D8 and Rigaku Ultima IV diffractometer equipped with Cu K_α (0.154 nm) radiation source. The primary excitation electron current was 40 mA at 40 kV for the characterization. The samples were scanned for 2θ values between 10^0 and 80^0. XRD spectra of LCPS embedded with different concentration of nanoparticle has been characterized.

Fourier Transform Infrared spectrometer Studies: Fourier Transform Infra-Red (FTIR) absorption spectra of pure LCPS and nanoparticles embedded in LCPS were recorded using Fourier Transform Infrared spectrometer (Bruker FTIR system) in the range varying between 4000 cm^{-1} and 400 cm^{-1}. By generating an infrared absorption spectrum, FTIR may determine the chemical bonds that make up a molecule. To determine chemical bonds, functional groups, and constituents of unidentified sample mixtures, one can utilise the FTIR infrared spectrometer approach.

Differential Scanning Calorimetry Studies: The transition temperatures of the substance were determined using differential scanning calorimetry (DSC). On a Perkin-Elmer Pyris 1 (Pyris Software version 7.0) instrument's equipment, DSC measurements were carried out. Nitrogen was pumped into the apparatus cell at a rate of 20 mL per minute. A 10 mL aluminium pan containing about 2-3 milligrammes of the substance was sealed hermetically.

IV. Results and Discussion

X-Ray Diffraction Studies: Figure 1, XRD spectrum of LCPS embedded with ZnO nanoparticle Sample-1(S1), showed the intense peaks at 2θ values of 31.84^0, 34.42^0, 36.24^0 and 40.36^0. The lines at d= 2.805 A^0(most intense), 2.6032 A^0 and 2.4758 A^0 corresponds to the ZnO and LCPS reflection. Traditional semi-crystalline polymers exhibit reflections and diffuse scattering in their crystalline and amorphous phases, respectively.

Figure 2, XRD spectrum of LCPS embedded with ZnO nanoparticle Sample-2(S2), showed the intense peaks at 2θ values of 31.80^0, 34.47^0 and 36.32^0. The lines at d= 2.4710 A^0 (most intense), 2.5997 A^0 and 2.8111 A^0 corresponds to the ZnO reflection.

Figure 3, XRD spectrum of LCPS embedded with ZnO nanoparticle Sample-3(S3), showed the intense peaks at 2θ values of 31.73^0, 36.32^0, 56.72^0 and 62.98^0. The lines at d= 2.4716 A^0 (most intense), 2.818 A^0 and 1.6215 A^0 corresponds to the ZnO reflection. The appearance of sharp reflections and diffuse scattering is characteristic of crystalline and amorphous phases of conventional semi-crystalline polymers.

Figure 4, XRD spectrum of LCPS embedded with ZnO nanoparticle Sample-4(S4), showed the intense peaks at 2θ values of 31.88^0, 34.41^0, 36.29^0 and 56.62^0. The lines at d= 2.4733 A^0 (most intense), 2.6043A^0 and 1.6242 A^0 correspond to the ZnO reflection. The crystal structure of ZnO nanoparticle was characterized by XRD pattern of ZnO NPs. The peaks at 2θ = 31.67^0, 34.31^0, 36.14^0, 47.40^0, 56.52^0, 62.73^0, 66.28^0, 67.91^0, 69.03^0 and 72.48^0 were assigned to (100), (002), (101), (102), (110), (200), (112), (201), and (004) of ZnO nanoparticles, indicating that the samples were polycrystalline (JCPDS 5-0664).

Figure 5, XRD spectrum of LCPS embedded with CuO nanoparticle Sample-1(S1), showed the intense peaks at 2θ values of 35.50^0, 38.63^0, 48.68^0, 61.49^0 and 67.98^0 . The lines at d= 2.3283 A^0(most intense), 2.5267 A^0 and 1.8687 A^0 correspond to the CuO and LCPS reflection.

Figure 6, XRD spectrum of LCPS embedded with CuO nanoparticle Sample-2(S2) showed the intense peaks at 2θ values of 35.61^0, 38.80^0 and 48.85^0. The lines at d= 2.3190 A^0 (most intense), 2.5191 A^0 and 1.8629 A^0 corresponds to the CuO and LCPS reflection.

Figure 7 XRD spectrum of LCPS embedded with CuO nanoparticle Sample-3(S3), showed the intense peaks at 2θ values of 35.62^0, 38.82^0, and 48.86^0. The lines at d= 2.5178 A^0 (most intense), 2.3173 A^0 and 1.8623 A^0 corresponds to the CuO reflection.

Figure 8, XRD spectrum of LCPS embedded with CuO nanoparticle Sample-4(S4), showed the intense peaks at 2θ values of 35.55^0, 38.73^0, 48.78^0, 61.59^0, 66.31^0 and 68.08^0. The lines at d= 2.5230 A^0 (most intense), 2.3225 A^0 and 1.8653 A^0 corresponds to the CuO reflection.

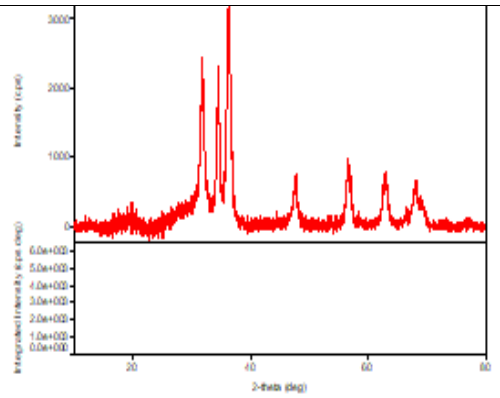

Figure 1: XRD spectrum of LCPS embedded with ZnO nanoparticles (S1)

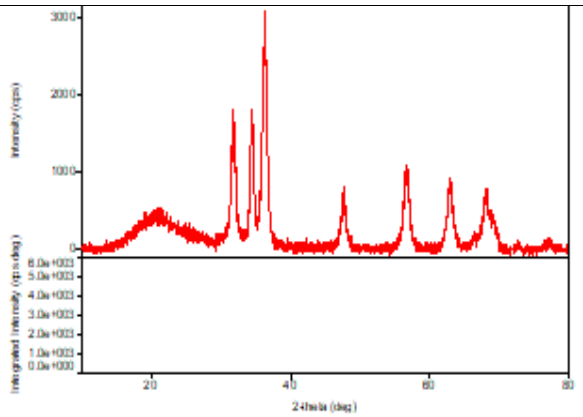

Figure 2: XRD spectrum of LCPS embedded with ZnO nanoparticles (S2)

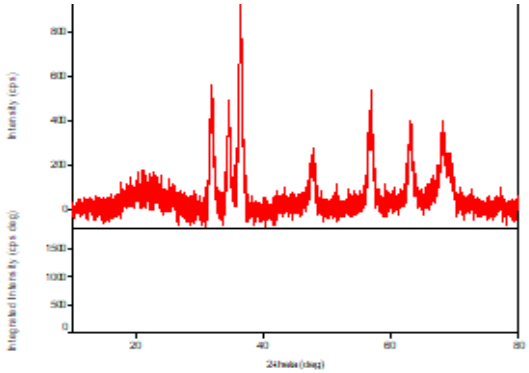

Figure 3: XRD spectrum of LCPS embedded with ZnO nanoparticles (S3)

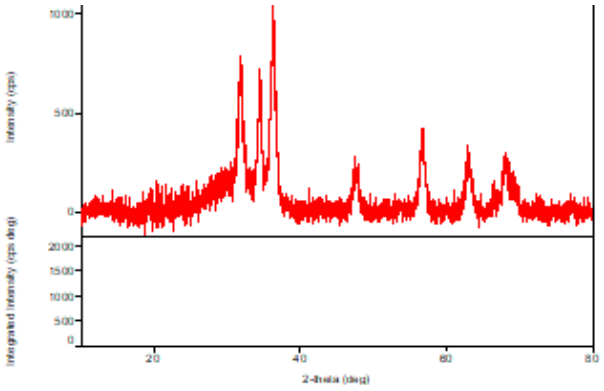

Figure 4: XRD spectrum of LCPS embedded with ZnO nanoparticles (S4)

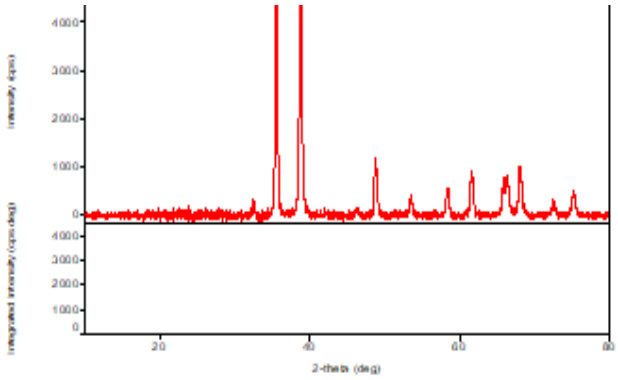

Figure 5: XRD spectrum of LCPS embedded with CuO nanoparticles (S1)

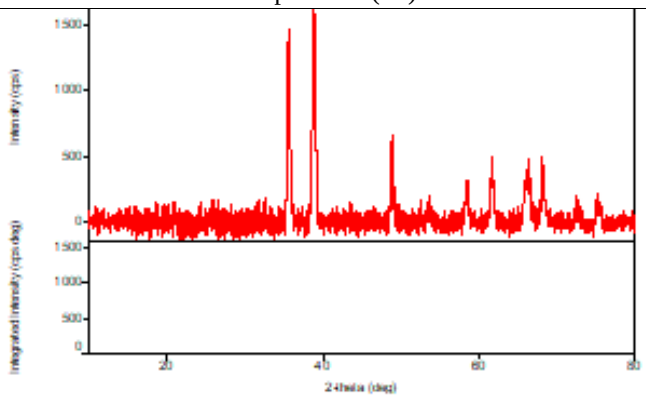

Figure 6: XRD spectrum of LCPS embedded with CuO nanoparticles (S2)

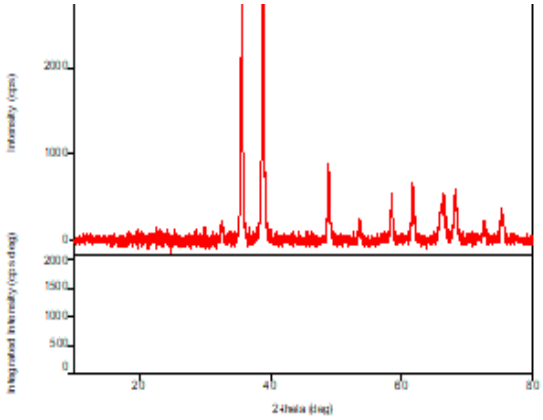

Figure 7: XRD spectrum of LCPS embedded with CuO nanoparticles (S3)

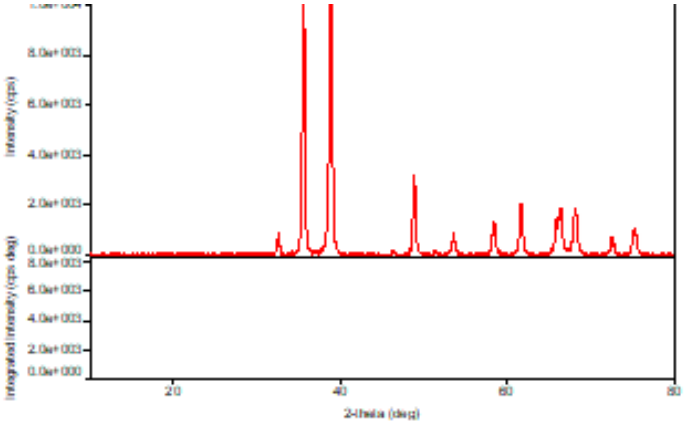

Figure 8: XRD spectrum of LCPS embedded with CuO nanoparticles (S4)

Figure 9, XRD spectrum of LCPS embedded with Zn nanoparticle Sample-1(S1), showed the intense peaks at 2θ values of 31.02^0, 36.33^0. The lines at d= 2.881 A^0 (most intense), 2.471 A^0 corresponds to the CuO and LCPS reflection.

Figure 10 XRD spectrum of LCPS embedded with Zn nanoparticle Sample-2(S2) showed the intense peaks at 2θ values of 36.05^0, 43.25^0 and 68.40^0. The lines at d= 2.090 A^0 (most intense), 2.489 A^0 Zn, and LCPS reflection.

Figure 11, XRD spectrum of LCPS embedded with Zn nanoparticle Sample-3(S3), showed the absence of peaks. This may be due to improper sample preparation. Figure 12, XRD spectrum of LCPS embedded with Zn nanoparticle Sample-4(S4), showed intense peaks at 2θ values of 31.80^0, 36.32^0, 39.06^0, 43.26^0, 56.55^0 and 62.80^0. The lines at d= 2.0895 A^0 (most intense), 2.471 A^0 and 2.8115 A^0 correspond to the Zn reflection.

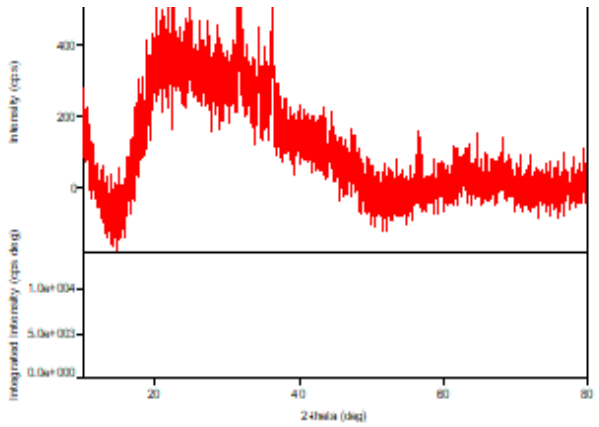

Figure 9: XRD spectrum of LCPS embedded with Zn nanoparticles (S1)

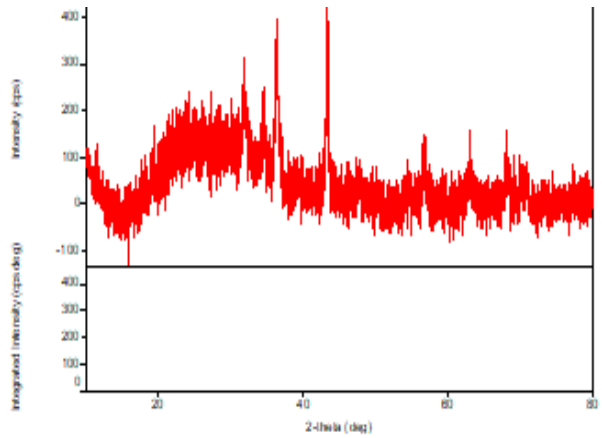

Figure 10: XRD spectrum of LCPS embedded with Zn nanoparticles (S2)

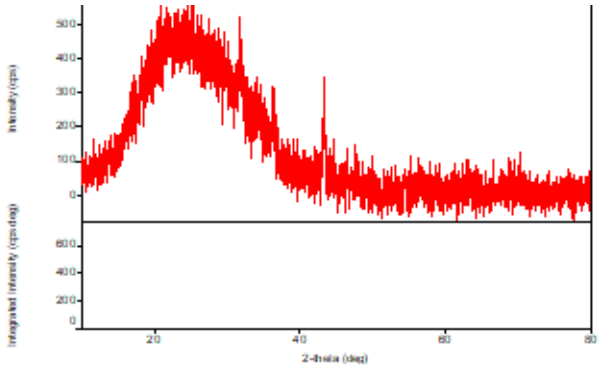

Figure 11: XRD spectrum of LCPS embedded with Zn nanoparticles (S3)

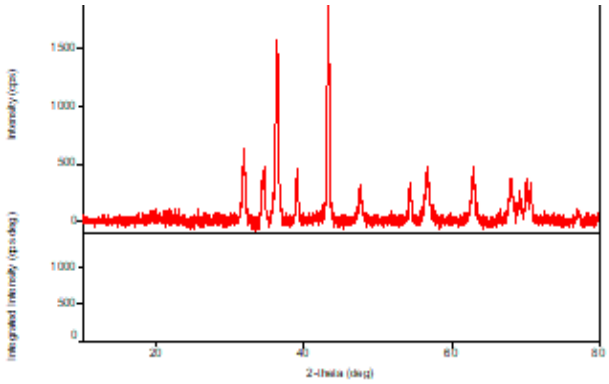

Figure 12: XRD spectrum of LCPS embedded with Zn nanoparticles (S4)

The results of LCPS embedded with different nanoparticle with different concentration showed sharp peak at different angles. XRD graph confirms the presence of ZnO, CuO and Zn nanoparticles in LCPS. The broadening of peaks revealed the size of the nanoparticles was in the order of nanometer. ZnO nanoparticles were added to the LCPS matrix, which improved the crystalline characteristics more than CuO and Zn nanoparticles implanted with LCPS.

Fourier Transform Infrared Spectrometer Studies

For pure LCPS, the peak present at 3382 cm^{-1} was due to O-H stretching of polymer and benzenoid rings and the peak present at 3026 cm^{-1} was due to C-H stretching shown in Figure 13. Similarly, the different peaks were obtained at different wavelengths for LCPS embedded with different concentration of ZnO nanoparticle are shown in Figure 14, Figure 15, Figure 16 and Figure 17. The combined graph is shown in Figure 18. The presence of phenyl liquid crystals is confirmed by the peak near 3500 cm^{-1} range.

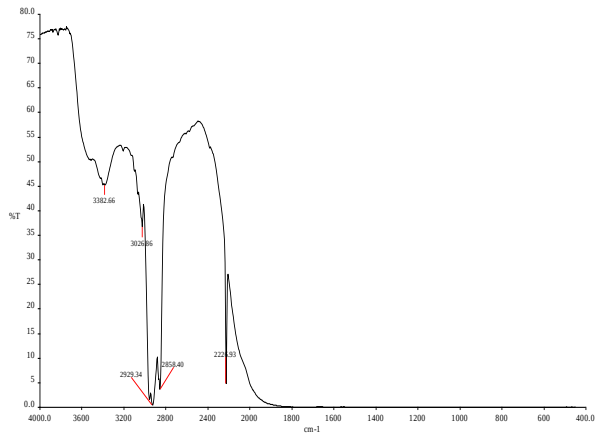

Figure 13: FTIR spectrum of pure LCPS (S0)

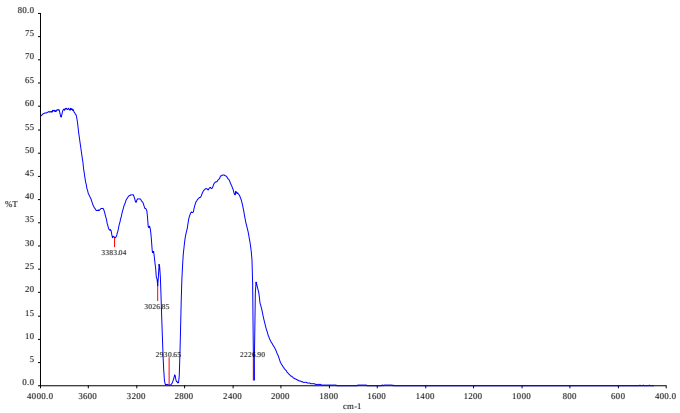

Figure 14: FTIR spectrum of LCPS embedded with 0.2% ZnO nanoparticles (S1)

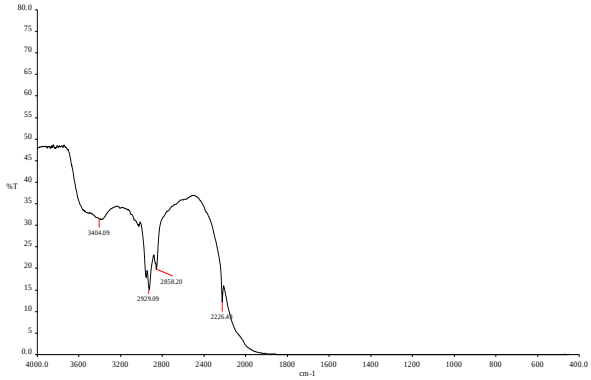

Figure 15: FTIR Spectrum of LCPS embedded with 0.5% ZnO nanoparticles (S2)

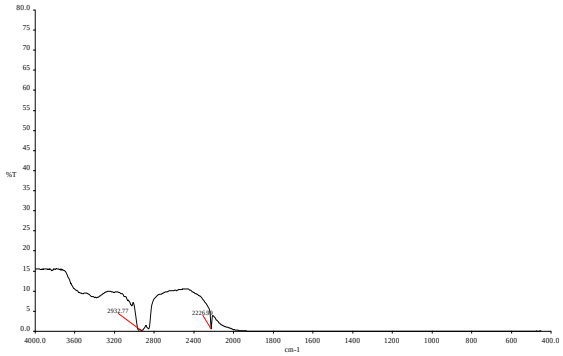

Figure 16: FTIR spectrum of LCPS embedded with 0.8% ZnO nanoparticle (S3)

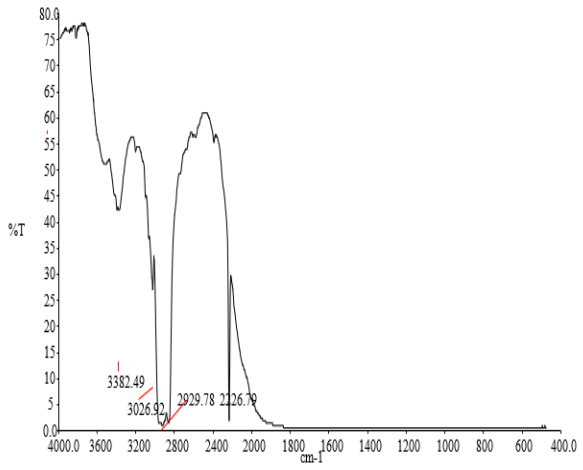

Figure 17: FTIR spectrum of LCPS embedded with 1.0% ZnO nanoparticles (S4)

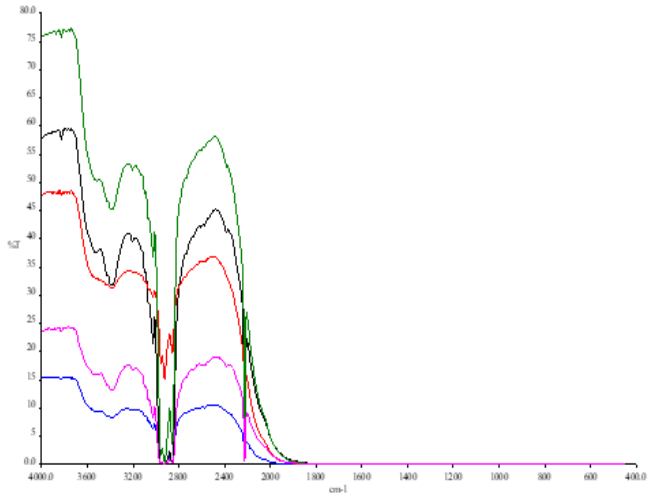

Figure 18: Combined FTIR spectrum of LCPS embedded with different concentration of ZnO nanoparticles

Differential Scanning Calorimetry Studies

The phase transition temperature for pure LCPS is 126^0C and maximum heat flow is 20.5 mW and is showed in Figure 19. The phase transition temperature for LCPS embedded with 0.2% ZnO nanoparticle is 138^0C and maximum heat flow is 21.13 mW as shown in Figure 20. The phase transition temperature for LCPS embedded with 1% ZnO nanoparticle is 154^0C and maximum heat flow is 23.75 mW as shown in Figure 21. The phase transition of LCPS embedded with 0.2% Zn nanoparticle is 125^0C, 142.5^0C and the value of maximum heat flow is 21.4 mW as shown in Figure 22. LCPS embedded with 0.3% Zn nanoparticle is 125^0C, 131^0C and value of maximum heat flow is 20.53 mW as shown in Figure 23. LCPS embedded with 0.5% Zn nanoparticle is 125^0C, 130^0C and value of maximum heat flow is 17.2 mW as shown in Figure 24. LCPS embedded with 0.8% Zn nanoparticle is 150^0C and value of maximum heat flow is 21 mW as shown in Figure 25. LCPS embedded with 1% Zn nanoparticle is 142^0C and value of maximum heat flow is 20.7 mW as shown in Figure 26. LCPS embedded with 0.4% CuO nanoparticle is 138^0C and value of maximum heat flow is 20.65 mW as shown in Figure 27. LCPS embedded with 0.5% CuO nanoparticle is 114^0C and value of maximum heat flow is 20.18 mW as shown in Figure 28.

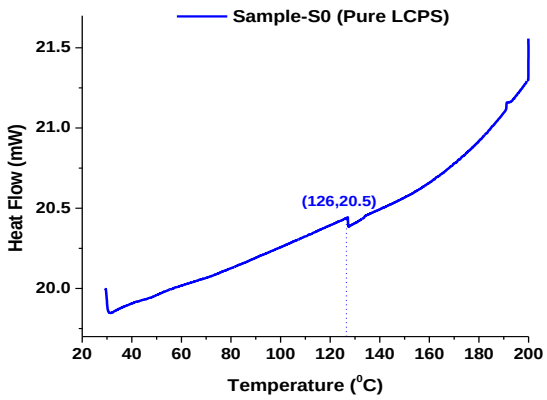

Figure 19: DSC graph of pure LCPS

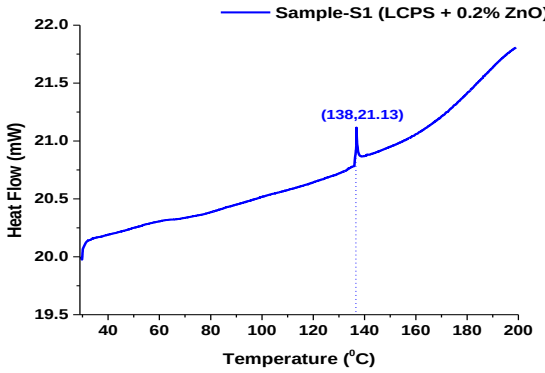

Figure 20: DSC graph of LCPS embedded with ZnO (S1)

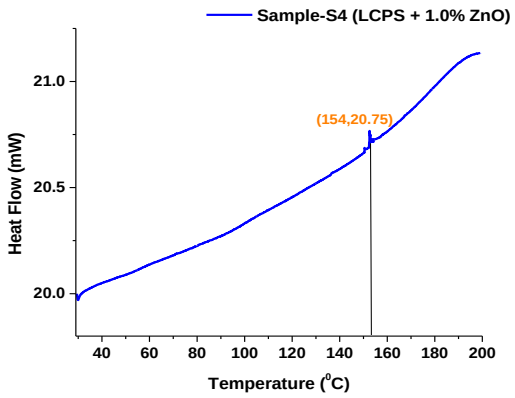

Figure 21: DSC graph of LCPS embedded with ZnO (S1)

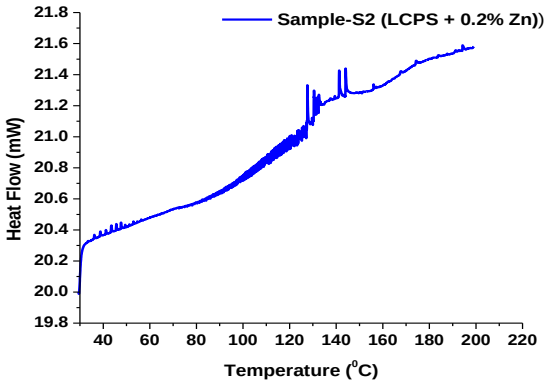

Figure 22: DSC graph of LCPS embedded with 0.2% Zn

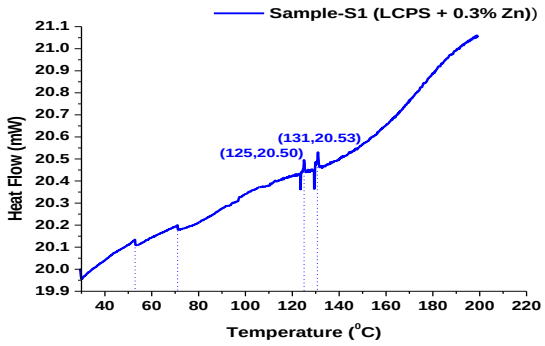

Figure 23: DSC graph of LCPS embedded with 0.3% Zn

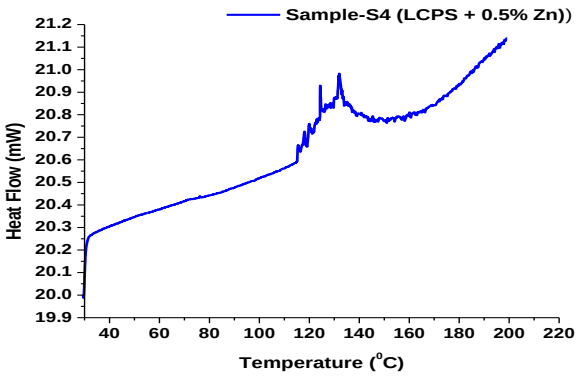

Figure 24: DSC graph of LCPS embedded with 0.5% Zn

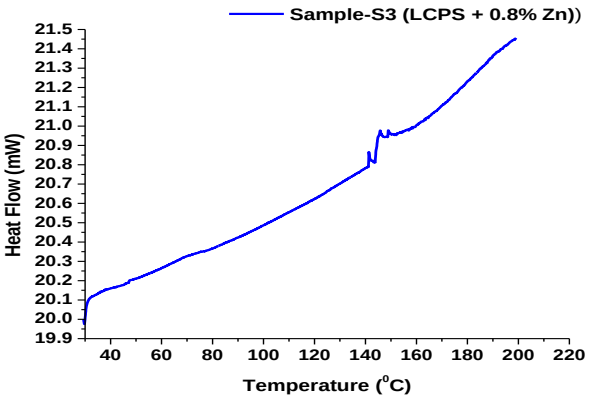

Figure 25: DSC graph of LCPS embedded with 0.8% Zn

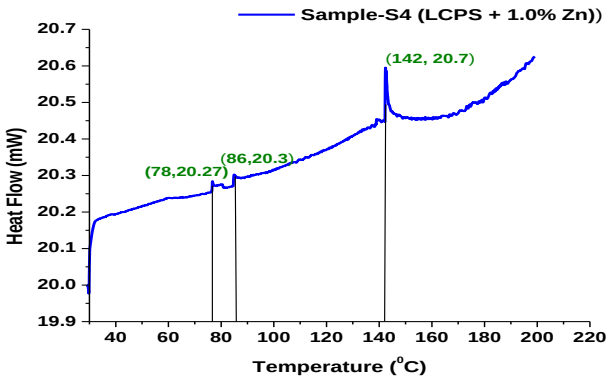

Figure 26: DSC graph of LCPS embedded with 1% Zn

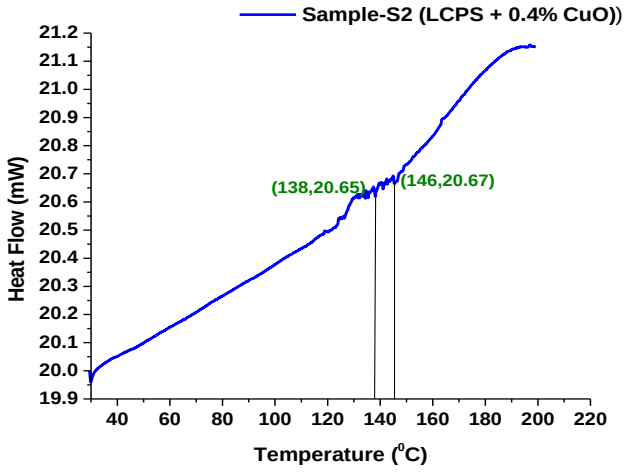

Figure 27: DSC graph of LCPS embedded with 0.4% CuO

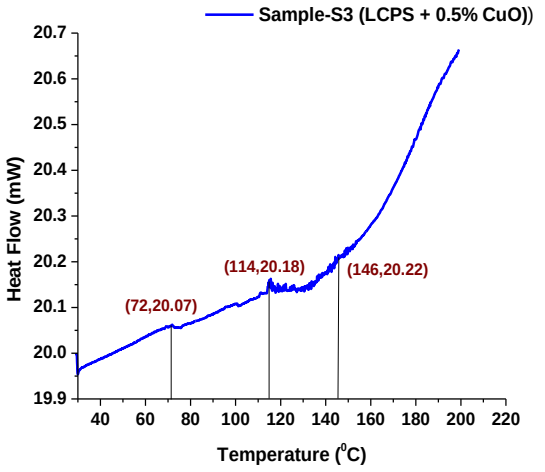

Figure 28: DSC graph of LCPS embedded with 0.5% CuO

Table 1 gives the comparison of phase transition temperature and heat flow characterzed by DSC for pure LCPS and LCPS embedded with different concentrations of ZnO , Zn, and CuO nanoparticles.

Table 1: Phase transition temperature measurement

Sr. No.	Name of Sample	Phase transition temperature	Heat flow (mW)
1.	Pure LCPS	126^{0}C	20.5
2.	LCPS + 0.2 % ZnO NP	138^{0}C	21.13
3.	LCPS + 1.0 % ZnO NP	154^{0}C	20.75
4.	LCPS + 0.2 % Zn NP	125^{0}C, 142.5^{0}C	21.4
5.	LCPS + 0.3 % Zn NP	125^{0}C, 131^{0}C	20.53
6.	LCPS + 0.5 % Zn NP	125^{0}C, 130^{0}C	17.2
7.	LCPS + 0.8 % Zn NP	150^{0}C	21
8.	LCPS + 1.0 % Zn NP	142^{0}C	20.7
9.	LCPS + 0.4 % CuO NP	138^{0}C	20.65
10.	LCPS + 0.5 % CuO NP	114^{0}C	20.18

Conclusions

ZnO nanoparticles significantly enhanced the crystalline properties of LCPS when compared to Zn and CuO nanoparticles. CuO nanoparticles implanted in LCPS function better than Zn nanoparticles placed in LCPS when it comes to electrical and electronic devices. The polymer phase with inorganic nanoparticles enhances the polymer matrix's thermal and mechanical stability. A better dopant for the creation of optically active LCPS materials is ZnO when compared to Zn and CuO. The optical and thermal properties of LCPS for use in displays are enhanced by ZnO nanoparticles.

References:

[1] S. Laschat, A. Baro, N. Steinke, F. Giesselmann, C. Hagele, G. Scalia, R. Judele, E. Kapatsina, S. Sauer, A. Schreivogel, M. Tosoni, Angew. Chem. Int. Ed. 46 (2007) 4832

[2] Shri Singh, “Liquid crystals fundamentals” by World Scientific Publishing Co. Pte. Ltd. ISBN 98102-4250-6, 2002.

[3] Abass, Aimi, et al. "Active liquid crystal tuning of metallic nano antenna enhanced light emission from colloidal quantum dots." Nano letters 14.10 (2014): 5555-5560.

[4] Rastogi, Ayushi, et al. "Study of an interesting physical mechanism of memory effect in nematic liquid crystal dispersed with quantum dots." Liquid Crystals 46.5 (2019): 725-735.

[5] Kuznetsova, Yulia V., et al. "Cadmium sulfide quantum dots in water media: Enhanced photoluminescence, dispersion and stability." Journal of Molecular Liquids 371 (2023): 121084.

[6] Pozhidaev, E. P., et al. "Polymer dispersed liquid crystals with electrically controlled light scattering in the visible and near-infrared ranges." Optical Materials Express 10.12 (2020): 3030-3040.https://doi.org/10.1364/OME.410163

[7] Subedi, Subhangi, et al. "Electrically Switchable Anisometric Carbon Quantum Dots Exhibiting Linearly Polarized Photoluminescence: Syntheses, Anisotropic Properties, and Facile Control of Uniaxial Orientation." ACS nano 16.4 (2022): 6480-6492.

[8] Yu, Meina, et al. "Luminescence enhancement, encapsulation, and patterning of quantum dots toward display applications." Advanced Functional Materials 32.13 (2022): 2109472.

[9] Mishra Krishnakant, Sheshmani K. Dubey, and Santosh A. Mani. "Optical characterization of inorganic nanoparticles doped in polymer dispersed liquid crystal." Molecular Crystals and Liquid Crystals 647.1 (2017): 244-252.

[10] Malik, P., & Singh, A. K. (2023). Metal oxide alumina nanowire-induced polymer-dispersed liquid crystal composites for low power consumption smart windows. *Journal of Molecular Liquids*, *378*, 121573.

[11] Zhang, Zhiwei, et al. "One-step microwave preparation of carbon dots-composited G-quartet hydrogels with controllable chirality and circularly polarized luminescence." Carbon 203 (2023): 39-46.

[12] Wang, Yijie, et al. "3D ZnO hollow spheres-dispersed CsPbBr3 quantum dots S-scheme heterojunctions for high-efficient CO2 photoreduction." Journal of Alloys and Compounds 945 (2023): 169197.

[13] Mani, S., Patwardhan, S., Hadkar, S., Mishra, K., & Sarawade, P. (2022). Effect of polymer concentration on optical and electrical properties of liquid crystals for photonic applications. *Materials Today: Proceedings*, *62*, 7035-7039.

[14] Priscilla, P., Malik, P., Kumar, A., Castagna, R., & Singh, G. (2023). Recent advances and future perspectives on nanoparticles-controlled alignment of liquid crystals for displays and other photonic devices. *Crit. Rev. Solid State Mater. Sci.*, *48*, 57.

[15] Smaisim, G. F., Mohammed, K. J., Hadrawi, S. K., Koten, H., & Kianfar, E. (2023). Properties and application of nanostructure in liquid crystals. *BioNanoScience*, *13*(2), 819-839.

[16] Saeed, M. H., Zhang, S., Cao, Y., Zhou, L., Hu, J., Muhammad, I., ... & Yang, H. (2020). Recent advances in the polymer dispersed liquid crystal composite and its applications. *Molecules*, *25*(23), 5510.

[17] Prakash, J., Khan, S., Chauhan, S., & Biradar, A. M. (2020). Metal oxide-nanoparticles and liquid crystal composites: A review of recent progress. *Journal of Molecular Liquids*, *297*, 112052.

[18] Mishra, K. G., Dubey, S. K., Mani, S. A., & Pradhan, M. S. (2016). Comparative study of nanoparticles doped in Liquid Crystal Polymer System. *Journal of Molecular Liquids*, *224*, 668-671.

[19] Zheng, Z., Xu, H., Wen, J., Chen, J., Mao, Z., Zhu, P., ... & Peng, J. (2024). In-situ growth of diamond/Ag as hybrid filler for enhancing thermal conductivity of liquid crystal epoxy. *Diamond and Related Materials*, *141*, 110659.

[20] Kumar, A., & Singh, G. (2024). Nanoparticles-induced alignment of nematic liquid crystals for tunable electro-optical devices. In *Advances in Fabrication and Investigation of Nanomaterials for Industrial Applications* (pp. 71-89). Cham: Springer International Publishing.

[21] Anan, S., Kurihara, T., Yamaguchi, M., Kikuchi, H., & Kokado, K. (2024). Enhanced Orientation of Liquid Crystals Inside Micropores of Metal–Organic Frameworks Having Thermoresponsivity. *Chemistry–A European Journal*, *30*(13), e202303277.

[22] Mani, S. A., Amare, J. R., Hadkar, S. U., Mishra, K. G., Pradhan, M. S., Al-Johani, H., & Sarawade, P. B. (2017). Investigations of optical and thermal response of polymer dispersed binary liquid crystals. *Molecular Crystals and Liquid Crystals*, *646*(1), 183-193.

[23] Wang, Y., Dang, A., Zhang, Z., Yin, R., Gao, Y., Feng, L., & Yang, S. (2020). Repeatable and reprogrammable shape morphing from photoresponsive gold nanorod/liquid crystal elastomers. *Advanced Materials*, *32*(46), 2004270.

[24] Guan, Z., Wang, L., & Bae, J. (2022). Advances in 4D printing of liquid crystalline elastomers: materials, techniques, and applications. *Materials Horizons*, *9*(7), 1825-1849.

[25] Mani, S., Patwardhan, S., Mishra, K., Hadkar, S., Khosla, S., & Sarawade, P. (2022, February). Wavelength and temperature dependent refractive index of polymer dispersed nematic liquid crystal. In *2022 First International Conference on Electrical, Electronics, Information and Communication Technologies (ICEEICT)* (pp. 1-4). IEEE.

[26] Wang, Y., Dang, A., Zhang, Z., Yin, R., Gao, Y., Feng, L., & Yang, S. (2020). Repeatable and reprogrammable shape morphing from photoresponsive gold nanorod/liquid crystal elastomers. *Advanced Materials*, *32*(46), 2004270.

[27] Zhang, Y., Chen, J., Hu, X., Zhao, W., Broer, D. J., & Zhou, G. (2021). Reverse mode polymer dispersed liquid crystal-based smart windows: A progress report. *Recent Progress in Materials*, *3*(4), 1-17.

[28] Chauhan, Garima, Praveen Malik, and Akash Deep. "Morphological, dielectric, electro-optic and photoluminescence properties of titanium oxide nanoparticles enriched polymer stabilized cholesteric liquid crystal composites." *Journal of Molecular Liquids* 376 (2023): 121406.

[29] Malik, Praveen, and Ashwani Kumar Singh. "Metal oxide alumina nanowire-induced polymer-dispersed liquid crystal composites for low power consumption smart windows." *Journal of Molecular Liquids* 378 (2023): 121573.

[30] Lu, Yinfu, et al. "Enhanced electro-optical properties of polymer-dispersed liquid crystals co-doped with fluorescent molecules and nanoparticles for multifunctional applications." *Chemical Engineering Journal* 485 (2024): 149654.

[31] Zhang, Cuihong, et al. "The regulation of electro-optical properties and polymer morphology of polymer-dispersed liquid crystal films with silicon nanostructure." *Liquid Crystals* (2024): 1-10.